Proceedings of the 4th African Rift Geothermal Conference 2012

Nairobi, Kenya, 21-23 November 2012

Computations in Real Rock - Heat Transport in 1/*K*-Noise Fractures

PC Leary, PE Malin & JA Pogacnik

Institute of Earth Sciences and Engineering
University of Auckland, Auckland New Zealand

p.leary@auckland.ac.nz

ABSTRACT

Heretofore the concept of geothermal heat transport has followed a rigid script dating from the early 70s. It features a mechanically quasi-uniform low-porosity/low-permeability clastic rock matrix that is either naturally or artificially riven by sundry quasi-planar megafractures supporting Poiseuille flow of *in situ* fluids. The origin and persistence of this fracture/flow concept is likely traceable to the visual identification of large-scale finite-width 'joints' in basement rock outcrops. Three serious problems, however, exist for 'joint' control *in situ* fluid flow. First, joint expansion seen in mechanical free-surface outcrops does not obviously apply at 3-5km-depth confining pressures. Second, attempts to identify wellbore evidence of 'active' interwell fracture-borne fluid pathways have not been conspicuously successful. Third, there is little evidence in well-log and/or well-core data for large-scale discrete mechanical fractures in an otherwise mechanically quasi-uniform rock matrix. Rather well-log and well-core evidence strongly favours a quite different physical relationship between the rock matrix, rock fractures, and *in situ* fluid flow. By joint prescription, wellbore microresistivity logs in an reservoir volume should record abrupt high-conductivity spikes as the resistivity sensor passes over conductive-fluid-containing joints. The power-spectrum of any spike sequence is essentially flat, $S(k) \sim 1/k^0 \sim const.$ In conspicuous contrast, microresistivity well-log data have, in common with the vast majority of geophysical well logs for most rock types and environments, Fourier power-spectra that scale inversely with wave number, $S(k) \sim 1/k^1$, over ~ 3 decades of scale range (generally ~1/Km < k < ~1/m, ~1/Dm < k < ~1/cm for microresistivity).

The systematic well-log power-law spectral scaling $S(k) \sim 1/k$ phenomenon that negates the matrix + megafracture reservoir concept of *in situ* flow opens the door on a scale-independent physical concept of *in situ* fractures, fluid flow and heat transport. Power-law scaling phenomena occur notably in thermodynamic binary-population order-disorder continuous phase transitions when an 'order parameter' reaches a 'critical value'. In rock, the

plausible critical-valued order parameter is grain-scale fracture density determined by the number of cement-disrupted/percolating grain-grain contact defects with in a host population of intact/non-percolating cement-bonded grain-grain contacts. As tectonic finite-strain deformation continually induces grain-scale failure of cement bonds in (clastic) rock, a critical-state percolation threshold value is maintained, rock volumes become percolation-permeable on scale lengths from mm to km, and well-log geophysical properties such as sonic wave speeds, electrical resistivity, soluble chemical species density, neutron porosity, and mass density fluctuations attain the power-law scaling fluctuation power-spectra $S(k) \sim 1/k$ observed over ~1/Km < k < ~1/cm. At the same time and by a closely related percolating grain-scale-fracture mechanism, *in situ* clastic rock attains a well-attested ~85% correlation $\delta\varphi \sim \delta\log(\kappa)$ recorded for spatial fluctuations in clastic reservoir well-core porosity φ and the logarithm of well-core permeability κ.

The observed physical conditions on *in situ* fractures and fluid flow $S(k) \sim 1/k$ and $\delta\varphi \sim \delta\log(\kappa)$ are straightforwardly incorporated into finite-element flow simulators. Flow simulations for 2D dense-grid realisations of permeable media obeying these spatial correlation systematics suggest that flow can proceed along 'pipe-like' structures. Laminar flow heat transport in pipes has a fixed Nusselt number $Nu \sim 4$. For a pipe of radius r flowing water at temperature ΔT from ambient, Newton's law of convective heat transport is $Q_{conv} = h\Delta T$, $[h]$ = W/m^2/^{o}C. Fourier's law of conductive heat transport for the same system is $Q_{cond} = K/r\Delta T$, $[K]$ = W/m/^{o}C. As $Nu \equiv Q_{conv}/Q_{cond}$, the coefficient of heat convection $h = 4K/r$ scales inversely with pipe radius r. Fracture-borne percolation could thus carry substantially more heat per flow mass than the large-pipe equivalents of reservoir planar-fracture flow models. Efficient heat transfer via pipe-like percolation could lead to much more compact reservoir volumes.

Finite-element 3D numerical flow/transport codes like *Sutra* can model a range of well-to-well percolation flow heat transport schema. Based on the forgoing considerations, we compact well-to-well heat transport models to the scale of a pair or quartet of horizontal parallel wellbores of length ℓ and offset $2a$ obey $\ell a^2 \sim 10^6$m^3, 100-1000 times smaller than generally conceived reservoir volumes. A pair of 1km-long parallel wellbores at ~50m offset can circulate fluid at wellbore flux ~25L/s and mean heat exchange volume percolation flow velocity ~10^{-8}m/s to notionally sustain ~1MWe power production per wellbore pair.

1. INTRODUCTION

In situ permeability has been a vexed issue in achieving, for example, Engineered/Enhanced Geothermal System power generation. By definition, EGS practice centres on increasing *in situ* permeability in a mass of low-permeability hot rock to extract commercial volumes of heat. Several decades of trial EGS projects in the US (Fenton Hill, 1970s), UK (Cornwall, 1980s), Europe (Soultz, 1990s) and Australia (Cooper Basin, Otway Basin, Paralana, 2000s) have, however, failed to demonstrate or develop the technology to generate heat

exchanger permeability volumes that allow commercially viable flow rates (Tester *et al.* 2006). Goldstein *et al.* (2011) cite generic failure to achieve adequate *in situ* flow as, along with the high cost of drilling, the major impediments to commercial EGS.

A likely underlying problem is not hard to identify. Abundant well-log and well-core data clearly indicate that *in situ* fluid flow is spatially far more heterogeneous at all scales than is generally allowed in hydrocarbon and geothermal reservoir concepts and flow models (Leary 2002; Leary & Walter 2008). It is thus more an article of faith than validated empirics that the details of *in situ* flow and flow heterogeneity in an reservoir heat exchange volume can be safely ignored via various averaging rubrics such as 'effective media', 'continuum mechanics', 'representative elementary volumes' or Thies/Earlougher pressure field interpretations (see, for instance, Ingebritsen, Sanford & Neuzil 2006; Sanyal & Butler 2005, 2010; Tester *et al*. 2006; Sutter *et al*. 2011).

From the earliest concepts of EGS (e.g., Gringarten *et al.* 1975), the prevailing assumption for *in situ* fracture mechanics and permeability stimulation is that the rockmass and its fractures are quasi-homogeneous in some technically meaningful sense. This assumption presumably has been informed in part by visual inspection of mines and outcrops (e.g., the Stripa project in Sweden, and downward projections of 'joints' seen in outcrop); in part by the hydrocarbon industry practice of averaging over smaller scale spatial variations to 'up-scale' to quasi-uniform (hence putatively predictable) estimates of reservoir flow parameters; and in part by a drive to overlook both the visible small-scale *in situ* spatial complications that are hard to define, and the seemingly haphazard large-scale spatial complications that defy systematic handling. The resulting 'abc's of standard reservoir flow modelling are thus:

a. rock as a mechanical continuum transected by (spatially uncorrelated) random distributions of meso- and macro-scale fractures that may or may not form flow networks;
b. fractures as discrete planar surfaces of mechanical discontinuity permitting laminar flow in 'effective' apertures;
c. application of high pressure wellbore fluids to part and/or connect meso- and macro-fractures for enhanced fracture permeability.

The following statement and sketch from Tester *et al.* (2006) illustrate the 'abc's:

"The volume of rock that can be fractured and the average spacing between the fractures, along with their length and width, will control the effective heat-exchange area of the reservoir."

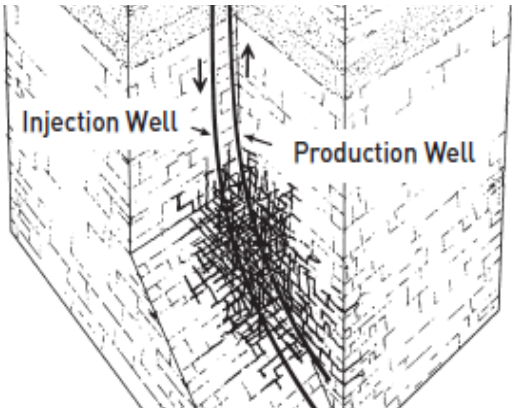

Figure 1: Cartoon of EGS fractures present in country rock and/or induced by wellbore pressurisation; the de facto assumptions are that rock is geomechanically homogeneous and fracture stimulation can be controlled for width, length, and spacing.

In some applications (e.g., Sanyal & Butler2005), effective media are given dual permeability in which the role of fractures is formalized into a secondary permeability superposed on continuum or matrix permeability:

"Improving permeability, without improving matrix-to fracture heat transfer area (that is, reducing fracture spacing), has little benefit in heat recovery or net generation."

The continuum approach to *in situ* fracture flow corresponds to hydrocarbon industry practice (Sayers & Schutjens 2007; Sayers 2007). It is questionable, however, that the practice of averaging over spatial complexity extends to reservoir flow modeling. With oil at ~50¢/L and hot water at ~0.5¢/L, geothermal wells must flow at 10 to 100 times the rate of oil wells to cover comparable drilling costs. While the hydrocarbon industry appears able to afford the cost of ignoring *in situ* flow spatial complexity, field-scale reservoir evidence indicates that the geothermal industry, particularly the important but as yet unrealized EGS sector, cannot.

We seek here to rectify this deficiency. We first characterise reservoir volumes in terms of heat transport in access wellbores and the heat exchange volume, and note that *in situ* permeability is by far the least constrained reservoir parameter. We then cite a range of field-scale evidence against *in situ* permeability homogeneity as in Fig 1, and present field-scale evidence for extensive and systematic *in situ* permeability heterogeneity. The latter evidence leads to the concept of *in situ* fluid flow as percolation via randomly fluctuating, long-range, spatially-correlated networks of fractures and fracture connectivity across the full range of scales from mm to Km. Numerical simulation of the observed spatial fluctuation systematics forms the basis for physically-accurate computing of EGS flow and heat transport on scales consistent with generic constraints on wellbore and heat-exchanger flow rates. Further developments in computation can begin to address the mechanics of

fracture stimulation needed to realise commercial power production.

2. SCALING EGS FLOW VOLUMES

EGS flow can be summarised in terms of two constraints on *in situ* fluid velocity v in the neighbourhood of a wellbore (Fig 2):

- Sufficiently high radial velocity $v(a)$ at wellbore radius a to power a turbine;
- Sufficiently low radial velocity $v(r)$ at radius r from the wellbore within the heat exchange volume to absorb heat at a sustainable rate.

Darcy's law connects spatially variable fluid velocity $\boldsymbol{v}$ to local permeability κ, fluid dynamic viscosity μ, and local pressure gradient,

$$\boldsymbol{v}(x,y,z) = \kappa(x,y,z)/\mu \nabla p(x,y,z). \qquad (1)$$

To estimate relative flow scales at EGS wellbore radius a relative to flow at inter-wellbore distance r in a spatially heterogeneous flow volume, we give Darcy's law a point-source/sink character,

$$\boldsymbol{v}(r) \sim \kappa(r)/\mu \, \partial r p(r), \qquad (1a)$$

centred on a point along the wellbore axis. The pressure field and gradient are then $P(r) = p_o r_o/r$ and $\partial r p \sim p_o r_o/r^2$, and local flow velocity at wellbore radius $r_o \sim a$ is $v(a) \sim \kappa/\mu \; p_o/a$. Flow per length into the wellbore circumference $2\pi a$ is then

$$Q(a)/\ell \sim 2\pi a \varphi v(a), \; (2)$$

where porosity φ governs how much of the rock volume conducts fluid. For (1a) as representative of flow along the wellbore length ℓ ~ 1000m, and with porosity φ ~ 10%, wellbore radius a ~ 10cm, wellbore pressure P_o ~ 1MPa, mean permeability κ ~ 1mD = 10^{-15}m^2, the fluid velocity at the wellbore is $v(a)$ ~ 0.1mm/s and total wellbore flow is Q ~ 6 10^{-3}m^3/s = 6L/s. The nominal electrical power gained from the wellbore flow

$$P = \varepsilon C Q \Delta T \qquad (3)$$

is then ~240kW for heat capacity C~ 4182J/L, ε ~ 10% conversion efficiency and ΔT ~ *100*^{o}C power cycle temperature drop.

Of the Fig 2 flow system parameters, by far the least constrained pertain to *in situ* permeability. We can use Fig 2 to identify a range of permeability unknowns needing discussion:

- On what scales to expect mean permeability values κ ~ 1mD = 10^{-15}m^2 required for acceptable EGS wellbore flow?
- What are the magnitude and distribution of variations about a mean permeability that could promote or retard achieving acceptable EGS wellbore flows over wellbore lengths ℓ ~ 1000m?
- What are the most natural means by which interwell flow in EGS volumes can be stimulated to achieve commercially viable power output?

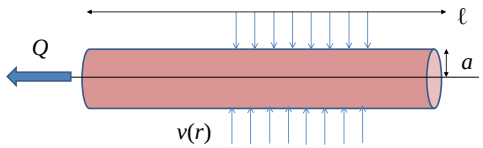

Darcy [m/s]: $v(a) = \kappa/\mu \, \partial_r P(a)$

Outflow [m^3/s]: $Q = 2\pi a \varphi v(a) \ell$

Power [MWe]: $P = \varepsilon c Q \Delta T$

Figure 2: Schema of EGS flow from country rock into wellbore. In situ flow velocity v [m/s] is given by Darcy's law for rockmass permeability κ[m2], in situ water dynamic viscosity μ [Pa-s], and pressure gradient ∂rP(r) [Pa/m]; wellbore outflow [m3/s] is given by rate of inflow over wellbore circumference 2πa [m] over length ℓ [m] allowing for in situ porosity φ; power [MWe] is given by wellbore outflow Q scaled to kg/s for water heat capacity c ~ 4[kJ/kg/oC], power cycle temperature drop ΔT [oC], and electrical power generation efficiency ε. For 1mD mean permeability κ ~ 10-15m2, in situ viscosity ~ 0.510-3 Pa-s, and nominal local pressure gradient 5 106Pa/m at wellbore radius a ~ 0.1m, mean flow velocity v ~ 10-4m/s = 0.1mm/s at the wellbore, giving Q ~ 6 10-3m3/s ~ 6kg/s for a 1km wellbore length if the rockmass porosity φ ~ 10%. For ε ~ 10% energy conversion efficiency over a ΔT ~ 100oC temperature power cycle drop, electrical power production is a nominal 240kWe per wellbore. Greater wellbore production effectively requires increasing EGS permeability.

3. *IN SITU* PERMEABILITY HETEROGENEITY

Responding to repeated failure to achieve standard EGS operations on crustal volumes using effective-medium/continuum/REV approximations to *in situ* fracture flow and fracture connectivity, we begin our permeability discussion with field-scale evidence that such approximations are poor over a considerable range of scale lengths. We then cite field-scale evidence for the type and degree of permeability heterogeneity encountered *in situ*.

3.1 Field Tests of Permeability Homogeneity

Evidence against permeability homogeneity exists at the volume scales of reservoirs, well intervals, and interwell intervals.

1.1 Whole EGS Volumes

The MIT 2006 report characterises the outcome of the 1970s Fenton Hill and 1980s Rosemanowes projects by citing joints as the key to EGS flow: 'the shearing of natural joints favourably aligned with the principal directions of the local stress field was a more important mechanism'; '.....researchers recognized that EGS reservoirs probably consisted of 3-dimensional networks of hydraulically activated joints and fractures....'; '.....a new technology related to the properties of any jointed rock mass.....'. Despite these suggestions, neither the Fenton Hill nor Rosemanowes projects approached commercial viability, nor supplied systematic evidence that joints were significant components of their respective EGS volume flow mechanics.

The MIT report goes on to state in the context of *in situ* joint flow that 'Recent progress at Soultz and Cooper Basin suggests that the ability to reach commercial levels is reasonably close.' It is immediately noticed, however, that neither the active tectonoseismic rift faulting at Soultz, nor the relic horizontal fracture system encountered in Cooper Basin (Glikson & Uysal 2010), are typical of EGS volumes. More relevant are the negative results of recent Cooper Basin and Paralana Hot Springs drilling and fracture stimulation projects: virtually no fracture stimulation or fluid injection in Cooper Basin granites at the Savina and Jolokia sites now abandoned as EGS prospects; absence of a once widely-subscribed notional compressive-stress-induced horizontal fracture system at Paralana; and Paralana fracture stimulation-induced seismic activity (Reid *et al.* 2011) similar in volume and character to that observed at Rosemanowes some 30 years earlier. There is no obvious or specific coherent support for *in situ* joint-flow in these data.

A more positive recent EGS volume result is the detection of a time-lapse electric resistivity signal at the Paralana site (Thiel *et al.* 2011). Some 3 million litres of water injected into a standard (~500m x 500m x 500m) EGS volume appear to have temporarily (~2 days) elevated the site *in situ* electrical conductivity at the well depth before the injected water was (presumably) absorbed into the rock mass. As no scenario of uniform take-up of the injected fluid in the central portion of the EGS volume seismicity cloud plausibly gives rise to a transient resistivity event, it is logical to assume the injected water was contained in, and transported away from the wellbore by, a large-scale natural fracture system. Such a fracture system need not, however, comprise 'joints'. Any sheet- or curtain-like fracture connectivity distribution implied by the induced seismicity that received a large volume of injected fluid would likely generate an MT time-lapse signal. Especially in light of the 2-day resistivity anomaly duration, a sufficient fluid distribution/dissemination scheme is given by the *in situ* multi-scale fracture-borne percolation pathway system outlined in the next section.

3.1.2 Single Well Volumes

Well-log spatial fluctuation systematics imply a very specific character to *in situ* fracture systems. That character is inconsistent with the existence of joints, at least as generally projected for EGS volumes. To see this, we take it that well-log electrical resistivity tools detect 'joints' intersected by the wellbore as high conductivity spikes arising from the extended connectivity of joint-borne brines relative to otherwise restricted brine connectivity of sealed pores. The spatial frequency power- spectrum $S(k)$ of a single spike, or any likely series of such spikes, is effectively constant, $S(k) \propto const$. In contrast, as illustrated in Fig 3 for an interval of clastic reservoir rock, actual micro-resistivity (FMI) logs measuring *in situ* resistivity with spatial resolution ~1mm have the characteristic spatial frequency power-spectrum of a large class of well-logs, $S(k) \propto 1/k$, over some 3.5 decades of scale length, ~1cycle/Hm < k < ~1cycle/dm (Leary 2002).

There is no systematic evidence in the Fig 3 sample wellbores of significant low resistivity spikes corresponding to discrete *in situ* fracture intervals or 'joints'; similar results obtain for clastic reservoir intervals elsewhere. The notable spikes in Fig 3 are resistivity highs associated with intervening shale bodies; there are few to no comparable resistivity lows. The observed high resistivity FMI spikes are embedded in a wideband range of scaling resistivity fluctuations that constitute the characteristic '1/*f*-noise' nature of well-log spatial variations (Leary 2002). We can thus infer from Fig 3 systematics that the classic 'joint' observed in outcrop is not a principal feature of *in situ* flow systems.

3.1.3 Interwell Volumes

Fig 3 and other FMI well-log spectra are evidence that large-scale joint-like *in situ* flow structures are likely to be more apparent to geologist's eye than real to *in situ* fluids. A parallel result was obtained in an attempt to establish a trial underground waste isolation volume at the Sellafield nuclear power facility in Cumbria, UK. In trying to detect well-to-well flow between a series of 1km deep wells in the regional country rock, UK Nirex concluded that

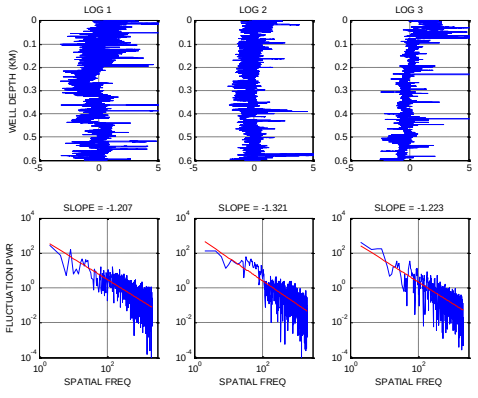

Figure 3: (Top) Three Formation Micro-Image (FMI) well logs taken at cm-spacing over a 600m interval of oil-field clastic reservoir analogue sand/shale sedimentary rock. Occasional well-log spikes are high resistivity shales rather than low resistivity sands or fractures; there is no significant presence of low resistivity spikes potentially corresponding to in situ fractures. (Bottom) FMI log power-

spectra; all spectra are power-law over some 1000 frequencies; power-spectral trends are inverse with spatial frequency, with exponents slightly larger than 1, typical of sedimentary media with significant sand/shale interfaces.

".....flow is undoubtedly principally through fractures but has been demonstrated to occur through only a small proportion. No direct and consistent association has been found between flow zones and any single geological characteristic...."
www.jpb.co.uk/nirexinquiry/nirex.htm

The UK Nirex conclusion is consistent with a considerable body of anecdotal evidence that well-to-well flow connectivity is anything but regular or characteristic of *in situ* flow.

3.2 Field Evidence for Large-Scale Permeability Heterogeneity

At the time that EGS was being first considered as a geothermal power option, Brace (1980) cited evidence for a number of cautions about the effective-medium/continuum approach to *in situ* permeability:

- *In situ* crystalline rock κ ~1-100mD
- No systematic decrease of κ with depth
- Over some interval at nearly every well κ ~ 1-100 mD to 2-3 km
- *In situ* permeability from earthquake precursors, anomalous pore pressures, aquifers leakages κ ~ 0.1 to 10 mD ~ permeable zones in wells
- *In situ* crystalline rocks κ ~10^3 times greater than for laboratory measurements
- For shale-rich rocks, laboratory, in situ, and inferred κ agree within factor ~ 10
- Laboratory study of artificial fractures suggest *in situ* values for crystalline rocks are high because of natural fractures; fractures may be sealed or absent in shale
  Re observed variation in wells, κ in crystalline rock not predictable within factor ~10^3
- Crystalline rock laboratory gives little more than minimum *in situ* κ
- For shale-rich rocks laboratory provide a good estimate of *in situ* κ
- Sensitivity of κ to effective stress implies measurement or estimation of κ must be tailored to stress
- If average crustal κ is about 10 mD, pore pressure much greater than hydrostatic ruled out for terrains of outcropping crystalline rocks; apart from hot pluton environments, anomalously high pore pressures require thick blanket of clay-rich rocks

3.2.1 Permeability Scaling at Outcrops

While Brace's cautions did not find their way into EGS literature, they have been amply justified by systematic observation of increasing *in situ* permeability (Fig 4) and a flow-related dispersion parameter (Figs 5-6) with increasing scale length.

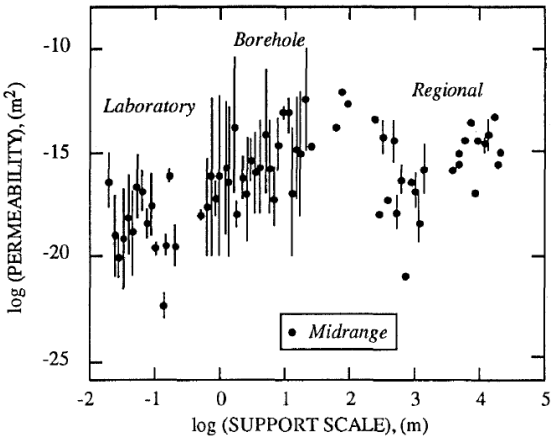

Figure 4: Observed permeability increase with increasing scale length for laboratory, wellbore, and outcrop scale ranges (Clauser 1992).

The dispersivity parameter plotted in Figs 5-6 measures how a chemical solute of concentration *c* disperses within a parcel of fluid flowing at velocity *v*. For longitudinal flow, $\partial_t c - v\partial_x c = \alpha v \partial_x^2 c$, dispersion α is a component of a diffusivity term αv, $[\alpha v] = m^2/s$. Dispersivity shares its scaling property with *in situ* velocity *v* proportional to permeability and hence scales with dimension more slowly (Figs 5-6) than permeability (Fig 4).

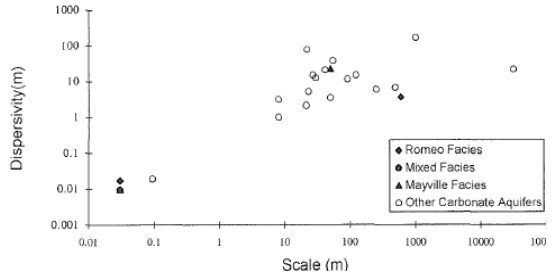

Figure 5: Observed longitudinal dispersivity increase with increasing scale length at outcrop scale (Schulze-Makuck & Cherhauer 1995).

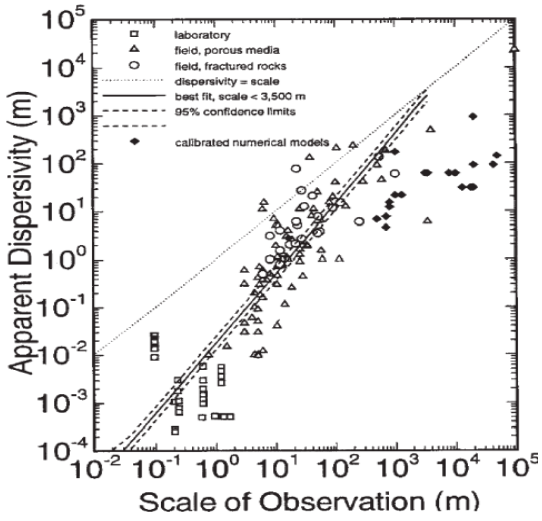

Figure 6: Observed longitudinal dispersivity increase with increasing scale length at outcrop scale (Neumam 1994, 1995).

These field data multi-decadal trends are direct evidence for systematic increase in ability of crustal rock to transport fluids as spatial dimensions increase. Increasing fluid transport capability with increasing scale implies a considerable degree of non-uniform flow in rock, and of course fundamentally invalidates the effective-medium/continuum approximation to *in situ* flow character. The observed trends are consistent with the systematic well-log evidence for higher amplitude fracture-density fluctuations at increasing scale as illustrated by Fig 3 micro-resistivity well-log power-spectra, and as detailed in the next section.

3.2.2 Spatial Variations in Well Productivity

Well productivity, the ability of wells to produce fluid from the surrounding rock, is observed to fluctuate strongly from well to well in the same reservoir formations, again re-enforcing the deficiency of effective-medium/continuum permeability approaches to *in situ* flow. Figs 7-9 summarise three instances of high degrees of *in situ* well flow variability from commercial geothermal and methane reservoir operations.

Fig 7 shows that geothermal well productivity for natural fracture systems in New Zealand is log-normally distributed (Grant 2009). Log-normal distributions directly contradict the effective-medium/continuum hypothesis which depends for its validity on at least approximate normal event distributions around a stable mean representative of the bulk scale. Histograms of the logarithm of well productivity data (Fig 7 right) show the width of well-productivity uncertainty. As in often the case with log-normal data, the variance is comparable to the mean. That is, deviations from the well-productivity mean are just as likely to be totally unproductive as highly productive. In fact, most geothermal power in New Zealand is produced from only a few highly productive wells; most geothermal wells are essentially a large drain on operational budgets.

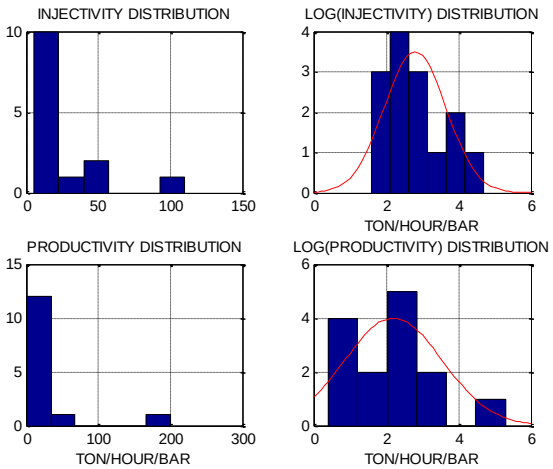

Figure 7: (Left) Log-normal distributions of selected New Zealand geothermal field well productivity and injectivity data; (right) normal distribution of the logarithm of these data (Grant 2009). Note that the distribution variances ~ the distribution means.

Fig 8 shows a variation on the same theme in the tight gas sand production wells of the Rulison field of western Colorado (Leary & Walter 2008). Wells drilled into a sequence of tight gas sands overlying coal measures are predicted to produce a given amount of methane based on the extent and type of sands traversed by each well. Fig 8 shows that observed production (vertical axis) is essentially independent of predicted production (horizontal axis). Simulations of the well-production prediction methodology show that the observed decoupling of prediction from actuality is consistent with the Fig 3 power-law scaling phenomenology detailed below (Leary & Walter 2008).

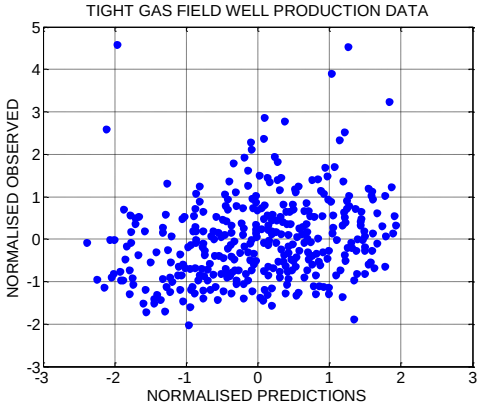

Figure 8: Predicted well methane production (horizontal axis) versus observed well production (vertical axis) for 250 wells in the Rulison gas field, western Colorado (Leary & Walter 2008).

Measurements of gas production for a single horizontal well in the coal-bed methane province of the Raton Basin in south-central Colorado in Fig 9 show variation along the well length in direct correlation with measured wellbore fracture density (Macartney & Morgan 2011). These well-specific productivity fluctuation data are consistent with the observed variable well productivity of Figs 7-8.

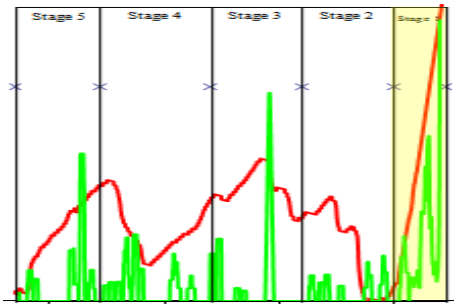

Figure 9: Variation of horizontal well gas production (red) as function of fracture content (green) along 800 meters of well length in Raton Basin, Colorado (Macartney & Morgan 2011).

4. *IN SITU* PERMEABIILITY AS PERCOLATION ALONG SPATIALLY-CORRELATED FRACTURE NETWORKS

Examination of well-log and well-core fluctuation systematics such as shown in Figs 10-11 provides direct evidence that, far from being 'effectively uniform' above some scale suitable length, fracture density, fracture-related porosity and fracture-related permeability systematically fluctuate on all scale lengths. The well-log and well-core empirical fluctuation properties can be summarised by the following bullets illustrated by Figs 10-12:

- Well-log power-spectra (Fig 10) show that *in situ* fracture density fluctuates inversely with spatial frequency from the scale of grains (mm) to that of reservoirs (km):

$$S(k) \sim 1/k. \qquad (4)$$

- Well-core sequences of porosity φ and permeability κ (Fig 11) show that zero-mean/unit-variance spatial fluctuations in porosity φ closely correlate with zero-mean/unit-variance spatial fluctuations in log(κ):

$$\delta\varphi \sim \delta\log(\kappa) \qquad (5)$$

- Permeability is typically log-normally distributed (Fig 12). Log-normal distributions largely arise from physical processes in which events are conditional on the product of (effectively) random variables rather than the sum of (effectively) random variables. Percolation flow along (spatially erratic) fracture pathways can be regarded as such a physical process. We can interpret the empirical relation (5) in terms of a normally distributed porosity distribution associated with a log-normally distributed connectivity distribution. If well-core porosity depends on fracture density n per unit volume, and well-core permeability depends on fracture connectivity probability $n!$ within that unit volume, then empirical poroperm fluctuation relation (5) reduces to a mathematical identity connecting normal randomness to log-normal randomness,

$$\delta n \sim \delta\log(n!). \qquad (6)$$

Well-log and well-core spatial fluctuation data sampled in Figs 10-12 attest to a fundamental character of *in situ* (clastic) crustal rock: finite-strain brittle fracture damage at grain-grain-cement contacts in crustal rock does not, as has been long assumed in geology, generate spatially uncorrelated distributions of grain-scale fractures, but instead generates long-range spatially-correlated fracture networks that interact on all scale lengths from grain-scale (mm) to reservoir scale (Km). The existence of long-range spatial correlations (e.g., meso- to mega-scale fracture systems) in a system of otherwise small-scale short-range interacting elements (e.g., grain-grain contacts) is known to characterise 'order-disorder critical-state phase transitions' in many physical systems (Leary 1997).

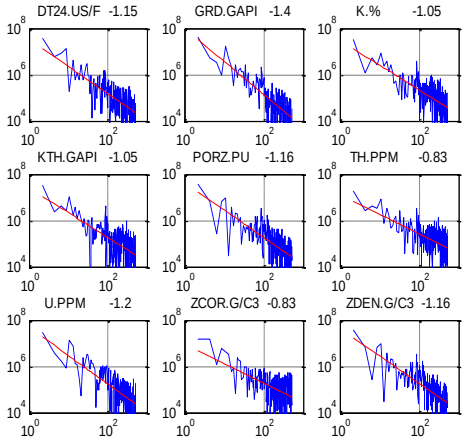

Figure 10: Power-law scaling power-spectra of a suite of well-log data recorded at a Wyoming hydrocarbon reservoir analogue site. Well-log spectra (blue) have straight-line fits (red) over 300 spectral values with slopes given above each plot; the mean slope is -1.13 ± 0.17. Well-log data courtesy of Slatt et al. 2006; cf Leary et al 2011; Leary 2002.

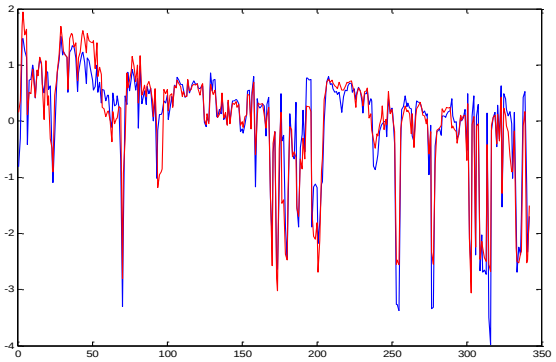

Figure 11: Fluctuation correlation between zero-mean/unit-variance porosity (blue) and zero-mean/unit-variance log(permeability) for a sequence of 350 well-core from tight gas sands formation in South Australia. Spatial correlation is 83%. Data courtesy of E Alexander, PIRSA. Cf Leary et al 2011; Leary & Walter 2008; Leary & Al-Kindy 2002.

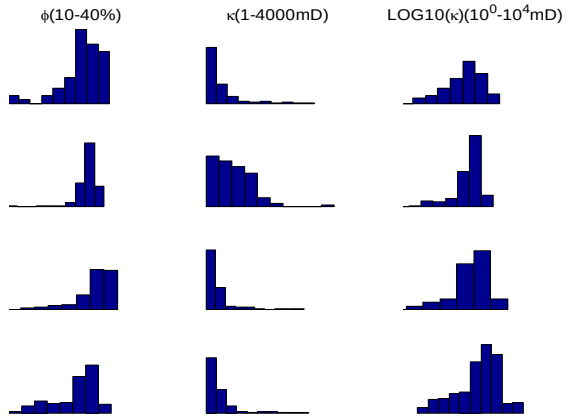

Figure 12: Sample poroperm probability distributions for well-core from Bierwang onshore North Sea gas field, Germany;(left column: porosity; middle column: permeability; right column log(permeability). Samples numbers are respectively 459, 67, 143, & 365. Range of distributions given on title line. Note similarity of porosity and log(permeability) distributions. Cf. Leary & Walter 2008, Leary & Al-Kindy 2002).

'Critical state' percolation is the simplest physical manifestation of order-disorder phase transition phenomenology (Stauffer & Aharony 1994). Fortunately it is straightforward to numerically simulation such distributions in 2 and 3 dimensions (Leary 2002). We now turn to numerical simulation of fluid flow as 'critical state' percolation through long-range spatially-correlated grain-scale fracture-connectivity pathways.

5. NUMERICAL SIMULATION OF PERCOLATION FLOW ALONG FRACTURE-CONNECTIVITY PATHWAYS

Fluid flow as percolation in a fractured poroperm medium characterised by empirical 'laws' (4)-(5) and intepreted via fracture-connectivity relation (6) has permeability spatial distribution

$$\kappa(x,y,z) = \kappa_0 \exp(\alpha\varphi(x,y,z)), \quad (7)$$

with κ_0 = bulk permeability and α = the ratio of standard deviations of $\log(\kappa(x,y,z))$ and $\varphi(x,y,z)$ distributions, $\alpha = \sigma(\log(\kappa(x,y,z)))/\sigma(\varphi(x,y,z))$. For well-log trajectory $s = s(x,y,z)$, the logarithm of (7) returns the empirical well-core poroperm fluctuation relation (5) illustrated in Fig 11, $\varphi(s)/\sigma(\varphi(s)) \sim \log(\kappa(s))/\sigma(\log(\kappa(s)))$. Fig 13 calibrates parameter α against the Fig 12 sample of well-core data from the North Sea gas sand reservoir formation shown. Visual reference to Figs 12-13 field data and frequency distributions indicates that $\alpha \sim 1$ is typical of clastic reservoir rock. For values $\alpha \sim 1$ the parameter is closely related to the standard deviation of log-normal distributions. In the context of *in situ* fluid flow, we note that standard deviations of mineral deposition frequency distributions are close to unity (Limpert, Stahel & Abbt 2001), suggesting that mineral deposition can (often) proceed by percolation flow in fracture systems .

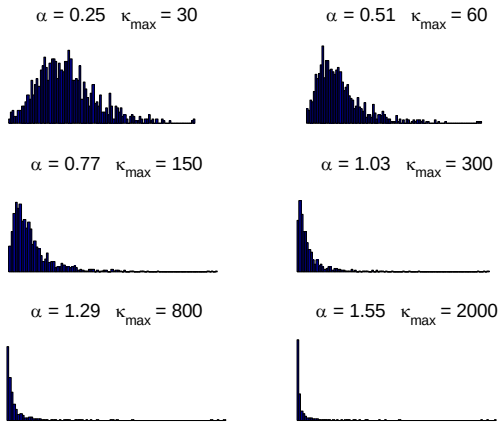

Figure 13: Numerical permeability distributions (7) as function random distributions of numerical porosity shaped by log-normal parameter α; values of $\alpha \sim 1$give log(permeability) distributions similar those observed for in situ core samples (Fig 12).

Diffusion of an incompressible fluid in a confined medium of permeability structure $\kappa(x,y,z)$ is given by the time-dependent Darcy's law,

$$1/B\partial_t P(x,y,z,t) = \nabla\cdot\boldsymbol{v}(x,y,z,t) = \nabla\cdot(\kappa(x,y,z)\nabla P(x,z,t)) \quad (8)$$

where B is effectively the porous medium elastic bulk modulusm (Ingebritsen, Sanford & Neuzil 2006). For covenience B is taken as constant.

Applying (8) to flow in 2D permeability media (7) generates steady state velocity fields $\boldsymbol{v}(x,z)$ illustrated in Figs 14-17 for sections of cross-well flow (see Leary & Malin 2011 for details). Bulk permeability κ_0 determines the overall time and pressure scales, while the log-normal shape parameter α determines the spatial distribution of percolation flow. Figs 14-15 illustrate quasi-uniform 2D velocity fields for small values of α while Figs 16-17 show the emergence of fracture-based flow paths as larger α increases fluid flow along connectivity channels corresponding to long-range spatially-correlated grain-scale fracture-density trends in line with well-log and well-core empirics (4)-(6).

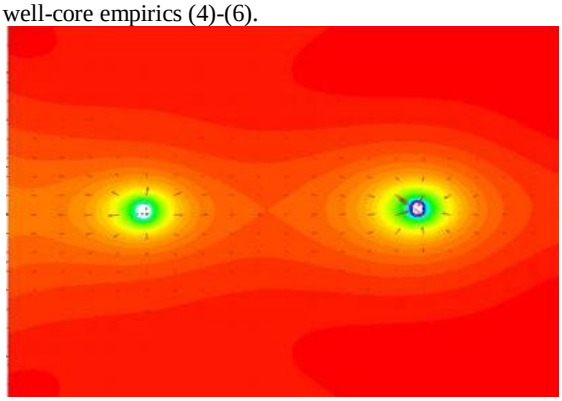

Figure 14: Quasi-uniform flow distribution in radial section of parallel wellbores for log-normal shape parameter α ~ 0.25.

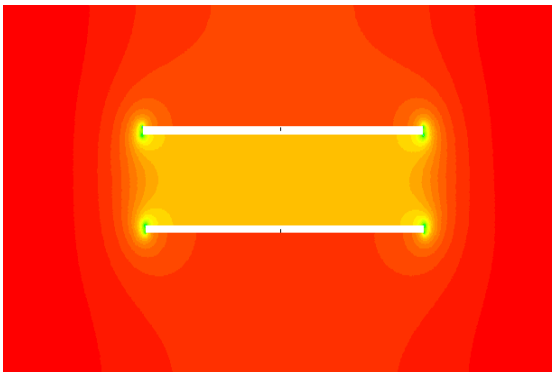

Figure 15: Quasi-uniform flow distribution in axial section of parallel wellbores for log-normal shape parameter α ~ 0.25.

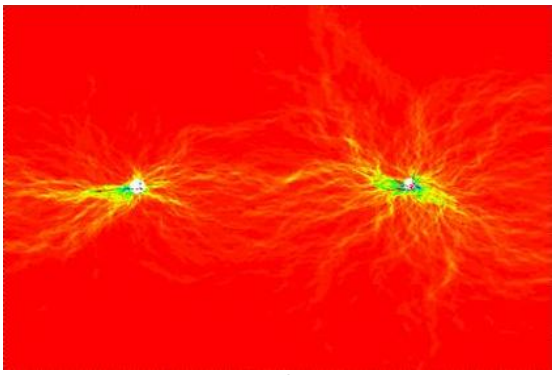

Figure 16: Fracture-based flow distribution in radial section of parallel wellbores for log-normal shape parameter α ~ 1.

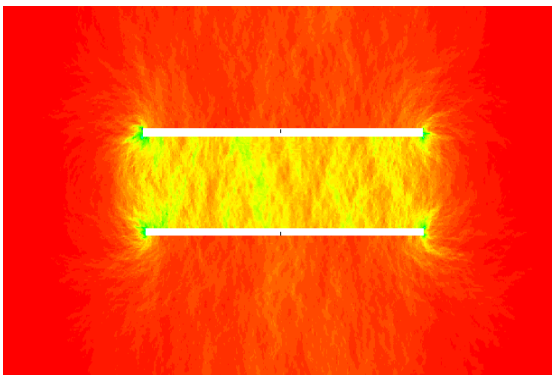

Figure 17: Fracture-based flow distribution in axial section of parallel wellbores for log-normal shape parameter α ~ 1.

The character of fluid flow in EGS heat exchange volumes is determined by the bulk permeability κ_0 and degree of fracture-borne flow governed by α. While bulk permeability is a standard flow parameter, of interest here is the perspective afforded by the fracture-based flow pictured in Figs 16-17 for log-normal shape parameter value α ~1. Fracture-dominated flow is characteristic of the commonplace log-normal permeability distributions such as sampled in Fig 12-13 for which α ~1 probability distributions are similar to observed well-core permeability probability distribution.

Understanding Fig 16-17 flow corresponding to fundamental aspects of *in situ* fracture distributions is likely to be key to developing EGS *in situ* permeability enhancement. A good deal of empirical observation is needed before we can accurately understand how to enhance the fracture content and connectivity of EGS volumes. However, a feature of immediate interest in Fig 16-17 flow distributions is the degree to which fracture-borne flow resembles flow in 'pipes'. While Figs 16-17 are 2D, 'pipe-flow' percolation permeability exists in 3D, with flow also following fracture-plane intersection pathways. In the context of generic wellbore-to-wellbore flow eqs (1)-(3), EGS heat transfer by 'pipe-flow' advection may reduce EGS modelling to a matter of flow decoupled from heat absorption and transfer.

6. EGS HEAT TRANSPORT AS ADVECTIVE 'PIPE-FLOW'

Laminar flow in a pipe has the property that its ability to transport heat is circumscribed by a constant. That constant is the dimensionless Nusselt number which for laminar pipe flow has value $Nu \sim 4$ (Rogers & Mayhew 1993). In particular, percolation flow in small pathway 'pipes' with diameter, say, ~1mm is laminar. Prompted by Figs 16-17 we consider the Nusselt number $Nu \sim$ const property of laminar pipe flow as might affect heat transport in a percolating EGS heat exchange volume.

Heat transport in pipes obeys Newton's law of heating/cooling, $Q_{conv} = h\cdot(T_w - T_s)$, where Q_{conv} is the watts per unit area of heat transport, h is a constant defined by the system geometry in units of W/m^2/^{o}C, T_w is the wellbore water temperature and T_s the ambient temperature in the surrounding rockmass. Heat flow by conduction in the same system obeys Fourier's law $Q_{cond} = K\cdot(T_w - T_s)$/r, where Q_{cond} is the watts per unit area of heat transport, r is the dimension over which heat is conducted -- in this case the pipe radius -- and K is the fluid thermal conductivity in units of W/m/^{o}C. By definition the ratio of the two pipe-borne heat transport values is Nusselt number $Nu = Q_{conv} / Q_{cond} \sim 4$. Cancelling the temperature term gives $Nu \sim 4 = hr/K$, fixing the forced-convection heat transfer coefficient $h \sim 4K/r$ as a function of pipe radius and (essentially constant) thermal properties of rock (all other things being equal for laminar flow). The smaller the pipe, the larger is the convective heat transport coefficient h and the more efficient the heat transfer.

By way of example, consider one pipe of radius $r_1 = r_0$ and four pipes of radius $r_2 = r_0/2$, each pipe flowing fluid at velocity v. The two pipe sets, one of radius r_1 and four of radius r_2, have the same mass flow, but different heat transport because of the different coefficients of heat transport:

$$W_1 = 1A_1vQ_1 = 1A_1vh_1\Delta T$$
$$W_2 = 4A_2v\ Q_2 = 4A_2vh_2\Delta T = A_1vh_2\Delta T, \qquad (9)$$

from which the ratio of heat transfer $W_1/W_2 = h_1/h_2 = r_2/r_1 = ½$; i.e., the four smaller pipes transport twice as much heat as the single larger pipe.

Heat flow efficiency considerations give a new perspective on the standard EGS model involving flow in a 'slab-fracture'. Consider, for instance, the model of Sutter *et al.* (2011) for heat transport via flow in a 30cm thick slab-fracture between two blocks of rock of dimension $\ell \sim 500$m. The model is cast in terms of heat transport in a 'square pipe' of 30cm on a side. Flow in the 'pipe' of velocity $v \sim 10^{-4}$ m/s is laminar (Reynolds number $v\ell/\mu = (10^{-4}$ m/s) (0.30m)/(1/2 10^{-6} m^2/s) ~ 60 << 5000 required for turbulence). Following the above 'pipe-flow' argument for a pipe 15cm radius versus a network of percolating pathways of comparable flow area suggests a large difference in heat transport efficiency in favour of percolation flow.

Heat transfer by fracture-borne percolation can be formally modelled to give more realistic estimates of the relative efficiency, but in general more efficient heat transport is preferable to less efficient heat transport. Focusing on efficiency, we can view with interest the EGS volume of eqs. (1)-(3) with length $\ell \sim 1000$m but having a much smaller cross-section involving heat transport by narrow-bore 'pipe-flow' as displayed in Figs 16-17. The 'efficient' EGS volume ~ 10^6 m^3 is ~1% of the standard EGS volume ~10^8m^3 most lately considered by Sutter *et al.* Much smaller EGS volumes offer the prospect of considerable savings along the path towards developing EGS fracture stimulation technology.

7. DISCUSSION/CONCLUSIONS

We propose reshaping the EGS wellbore-to-wellbore flow problem along the lines of a fracture-borne fluid percolation flow based on empirical *in situ* permeability properties of crustal rock (4)-(7).

Application of EGS flow-velocity constraints (1)-(3) compatible with commercial wellbore flow and sustainable heat extraction from the EGS volume imply that sustainable commercial heat extraction of order 1MW$_e$ per horizontal parallel wellbore pair is possible in EGS heat exchange volumes of size 10^{-6}m^3, ~1% of standard volumes. Smaller EGS volumes arise from more efficient heat extraction for fluids percolating though an EGS volume than for fluids flowing along slab-fractures imposed on the volume.

Fracture-based fluid percolation through significantly smaller EGS volumes has a number of advantages for developing the technology to generate viable EGS flow systems:

- Empirically validated *in situ* percolation flow scenarios offer more physically realistic approaches to stimulating *in situ* fractures in the inter-wellbore EGS volume;
- Fracture-based percolation flow suggests that low-pressure fracture stimulation of existing fractures is more effective than high-pressure stimulation seeking to impose fractures on the existing fracture fabric;
- Smaller EGS volumes have significant cost-reduction implications for conducting detailed wellbore-based investigations of fracture stimulation;
- Smaller EGS volumes and lower stimulation pressures reduce earthquake hazards;
- Use of highly instrumented long-reach horizontal well-pair stimulation volumes of order 10^6m^3 tracks current drilling and fracking technology;
- Understanding an EGS fracture-percolation-based permeability stimulation process is of direct interest to the hydrocarbon industry for greater well productivity and the mining industry for better understanding of roof-collapse mining techniques;
- Provides a basis for more physically accurate computation of fracture stimulation; Fig 18 shows flow paths for a low-resolution 2D multi-well EGS flow system designed to run at negative net pressure relative to ambient pressure to reduce loss of injector well fluids; parallelising the code can extend the fracture-stimulation to higher grid resolution in 3D.

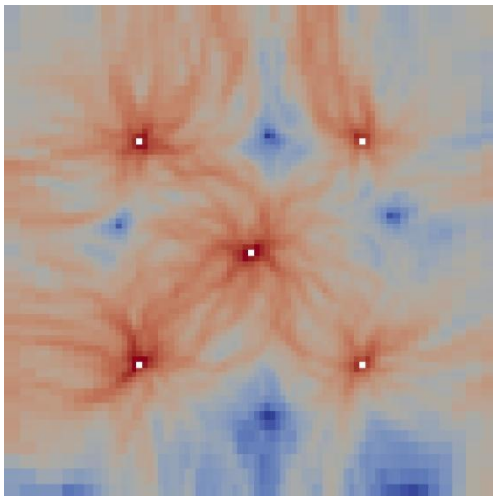

Figure 18: Fracture-based flow distribution in radial section of five parallel wellbores for log-normal shape parameter $\alpha \sim 1$; a central wellbore supplies heat-depleted water from the surface to the EGS volume; the surrounding quartet of wellbore returns heat charged water to the surface; all wellbore run a pressures below ambient in order to avoid fluid loss into the surrounding rock volume fracture set (Pogacnik, Leary & Malin 2011).

REFERENCES

Brace WF (1980) Permeability of crystalline and argillaceous rocks, *International Journal of Rock Mechanics, Mineral Science. & Geomechanics Abstracts* 17, 241-251.

Clauser C (1992) Permeability of crystalline rocks, *EOS Transactions AGU* 73 No 21, 233-237.

Glikson AY & Uysal IT (2010) Evidence of impact shock metamorphism in basement granitoids, Cooper Basin, South Australia, *Proceedings*

Australian Geothermal Energy Conference, Adelaide SA, 16-18 November.

Goldstein BA, Hiriart G, Tester J, Bertani B, Bromley C, Gutierrez-Negrin L, Huenges E, Ragnarsson A, Mongillo M, Muraoka H & Zui VI (2011) Great expectations for geothermal energy to 2100, *Proceedings 36th Workshop on Geothermal Reservoir Engineering*, Stanford University, January 31-February 2.

Grant MA (2009) Optimization of drilling acceptance criteria, *Geothermics* 38, 247–253.

Gringarten AC, Witherspoon PA *et al.* (1975) Theory of Heat Extraction from Fractured Hot Dry Rock, *Journal of Geophysical Research* 80, 1120-1124.

Ingebritsen SE, Sanford WE & Neuzil CE (2006) *Groundwater in Geologic Processes*, 2nd ed., Cambridge University Press, Cambridge UK, pp655.

Leary PC (1997) Rock as a critical-point system and the inherent implausibility of reliable earthquake prediction, *Geophysical Journal International* 131, 451-466.

Leary PC (2002) Fractures and physical heterogeneity in crustal rock, in *Heterogeneity of the Crust and Upper Mantle – Nature, Scaling and Seismic Properties*, J. A. Goff, & K. Holliger (eds.), Kluwer Academic/Plenum Publishers, New York, 155-186.

Leary PC & Al-Kindy F (2002) Power-law scaling of spatially correlated porosity and log(permeability) sequences from north-central North Sea Brae oilfield well core, *Geophysics Journal International* 148, 426–442.

Leary P & Malin P (2011) Is Theis flow modelling sufficient for EGS/HSA geothermal energy production? *Proceedings 37th Geothermal Resources Council Conference*, San Diego CA, 23-26 October 2011.

Leary P & Malin P (2011) MW_{th} ~ 4ΔT(C)/1000 Q(L/s) -- Scaling heat transport to in situ flow velocity10^{-8} m/s for 100 L/s wellbore flow in fractured media, *Proceedings AAPG/SPE/SEG Hedberg Conference "Enhanced Geothermal Systems"* – Napa CA, 14-17 March.

Leary PC & Walter LA (2008) Crosswell seismic applications to highly heterogeneous tight-gas reservoirs, Special Topic on Tight Gas, *First Break* 26, 33-39.

Leary PC, Malin PE, Pogacnik J & Macartney H (2011) Well Log and Core Based 3D EGS Flow Simulation – Application to the Raton Basin Thermal Anomaly, CO, USA, *Proceedings Australian Geothermal Energy Conference*, Melbourne 16-18 November 2011.

Limpert E, Stahel WA & Abbt M (2001) Log- normal distributions across the sciences: Keys & clues, *Bioscience* 51, 341-352.

Macartney H & Morgan P (2011) The Potential for Geothermal Energy Recovery from Enhanced Geothermal Systems in the Raton Basin of Southern Colorado, USA, *Proceedings AAPG/SPE/SEG Hedberg Conference "Enhanced Geothermal Systems"* – Napa CA, 14-17 March.

Neuman SP (1994) Generalized scaling of permeabilities: Validation and effect of support scale, *Geophys. Res. Lett.* 21, 349–352.

Neuman SP (1995) On advective dispersion in fractal velocity and permeability fields, *Water Resources Research* 31, 1455–1460.

Pogacnik J, Leary P & Malin P (2011), Implementation and numerical analysis of fully-coupled non-isothermal fluid flow through a deformable porous medium, Proceedings NZ Geothermal Workshop, Auckland 21-23 November.

Reid PW, Messeiller M, Llanos EM & Hasting M (2011) Paralana 2 – Well Testing and Stimulation, *Proceedings Australian Geothermal Energy Conference*, Melbourne,. 16-18 November.

Rogers G & Mayhew Y (1993) *Engineering Thermodynamics Work and Heat Transfer*, Longman Scientific& Technical, Essex UK, 711pp.

Rock Characterisation Facility at Longlands Farm, Gosforth, Cumbria; Assessor's Report -- Appeal by UK Nirex – *www.jpb.co.**uk/nirex**inquiry/**nirex**.htm*

Sanyal SK & Butler SJ (2005) An Analysis of Power Generation Prospects from Enhanced Geothermal Systems, *Proceedings World Geothermal Congress 2005*, Antalya, Turkey, 24-29 April.

Sanyal SK & Butler SJ (2010) Geothermal Power Capacity of Wells in Non-Convective Sedimentary Formations, *Proceedings World Geothermal Congress 2010*, Bali, Indonesia, 25-29 April.

Sayers CM & Schutjens PMTM (2007) Geomechanics: Special Section, *The Leading Edge* 26, 582-662.

Sayers CM (2007) Fractures: Special Section, *The Leading Edge* 26, 1102-1202.

Schulze-Makuck D & Cherhauer DS (1995) Relation of hydraulic conductivity and dispersivity to scale of measurement in a carbonate aquifer, In: Models for Assessing and Monitoring Groundwater Quality, ed. By B.J. Wagner, T. H. Illangasekare & K. H. Jensen, IAHA Publication No. 227.

Slatt, RM, Minken J, Van Dyke SK, Pyles DR, Witten AJ & Young RA (2006) Scales of Heterogeneity of an Outcropping Leveed-channel Deep-water System, Cretaceous Dad Sandstone Member, Lewis Shale, Wyoming, USA, *in* T. H. Nilsen, R. D. Shew, G. S. Steffens, and J. R. J. Studlick, eds., *Atlas of Deep-Water Outcrops: AAPG Studies in Geology* 56.

Stauffer D & Aharony A (1994) *Introduction to Percolation Theory*, Taylor & Francis, London, 181pp.

Sutter D, Fox DB, Anderson BJ, Koch DL, von Rohr PR &Tester JW (2011) Sustainable heat farming of geothermal systems: a case study of heat extraction and thermal recovery in a model egs fractured reservoir. *Proceedings 36th Workshop on Geothermal Reservoir Engineering*, Stanford University, January 31-February 2.

Tester JW *et al.* (2006), *The Future of Geothermal Energy -- Impact of Enhanced Geothermal Systems (EGS) on the United States in the 21st Century*, Massachusetts Institute of Technology, 372pp.

Thiel S, Peacock J, Heinson G, Reid P & Messeiller M (2011) First results of monitoring fluid injection in EGS Reservoirs Using Magnetotellurics, *Proceedings Australian Geothermal Energy Conference*, Melbourne,. 16-18 November.